



# Invariant NKT cells metabolically adapt to the acute myeloid leukaemia environment

Victoria Stavrou<sup>1</sup> · Livingstone Fultang<sup>1</sup> · Sarah Booth<sup>1</sup> · Daniele De Simone<sup>1</sup> · Arekdiusz Bartnik<sup>1</sup> · Ugo Scarpa<sup>1</sup> · Luciana Gneo<sup>1</sup> · Silvia Panetti<sup>1</sup> · Sandeep Potluri<sup>2</sup> · Meaad Almowaed<sup>3</sup> · Jonathan Barlow<sup>4</sup> · Andris Jankevics<sup>5</sup> · Gavin Lloyd<sup>5</sup> · Andrew Southam<sup>5</sup> · David A. Priestman<sup>6</sup> · Paul Cheng<sup>7</sup> · Warwick Dunn<sup>2,8</sup> · Frances Platt<sup>6</sup> · Hitoshi Endou<sup>9</sup> · Charles Craddock<sup>2</sup> · Karen Keeshan<sup>3</sup> · Francis Mussai<sup>1</sup> · Carmela De Santo<sup>1</sup>

Received: 18 February 2022 / Accepted: 27 July 2022 / Published online: 13 August 2022  
© The Author(s) 2022

## Abstract

Acute myeloid leukaemia (AML) creates an immunosuppressive environment to conventional T cells through Arginase 2 (ARG2)-induced arginine depletion. We identify that AML blasts release the acute phase protein serum amyloid A (SAA), which acts in an autocrine manner to upregulate ARG2 expression and activity, and promote AML blast viability. Following in vitro cross-talk invariant natural killer T (iNKT) cells become activated, upregulate mitochondrial capacity, and release IFN- $\gamma$ . iNKT retain their ability to proliferate and be activated despite the low arginine AML environment, due to the upregulation of Large Neutral Amino Acid Transporter-1 (LAT-1) and Argininosuccinate Synthetase 1 (ASS)-dependent amino acid pathways, resulting in AML cell death. T cell proliferation is restored in vitro and in vivo. The capacity of iNKT cells to restore antigen-specific T cell immunity was similarly demonstrated against myeloid-derived suppressor cells (MDSCs) in wild-type and  $\text{J}\alpha 18^{-/-}$  syngeneic lymphoma-bearing models in vivo. Thus, stimulation of iNKT cell activity has the potential as an immunotherapy against AML or as an adjunct to boost antigen-specific T cell immunotherapies in haematological or solid cancers.

**Keywords** iNKT · AML · ASS · LAT-1 · Arginine · Cancer

## Introduction

T cell immunotherapies, notably chimeric-antigen receptor T (CAR-T) cells against CD19 or CD22 on acute lymphoblastic leukaemia (ALL) blasts, have demonstrated the potential to generate clinically significant immune responses in

haematological malignancies [1]. However, in AML activating T cell immunity against blasts remains challenging. Strategies to induce T cell cytotoxicity against AML blasts including upregulation of peptide antigen presentation, release of T cells from immune checkpoint inhibition, and engineering of antigen-specific or chimeric-antigen receptors have not consistently demonstrated activity in clinical trials [2–4].

Carmela De Santo and Francis Mussai contributed equally to this manuscript as senior authors.

✉ Francis Mussai  
francis.mussai@nhs.net

<sup>1</sup> Institute of Immunology and Immunotherapy, University of Birmingham, Birmingham B15 2TT, UK

<sup>2</sup> Institute of Cancer and Genomics, University of Birmingham, Birmingham B15 2TT, UK

<sup>3</sup> Paul O’Gorman Leukaemia Research Centre, University of Glasgow, Glasgow G12 0YN, UK

<sup>4</sup> School of Sport, Exercise and Rehabilitation Sciences, University of Birmingham, Birmingham B15 2TT, UK

<sup>5</sup> School of Biosciences and Phenome Centre Birmingham, University of Birmingham, Birmingham B15 2TT, UK

<sup>6</sup> Department of Pharmacology, University of Oxford, Oxford OX1 3QT, UK

<sup>7</sup> Bio-Cancer Treatment International, Hong Kong Science Park, Hong Kong, China

<sup>8</sup> Institute of Metabolism and Systems Research, University of Birmingham, Birmingham B15 2TT, UK

<sup>9</sup> J-Pharma Co. Ltd, Yokohama, Kanagawa 230-0046, Japan

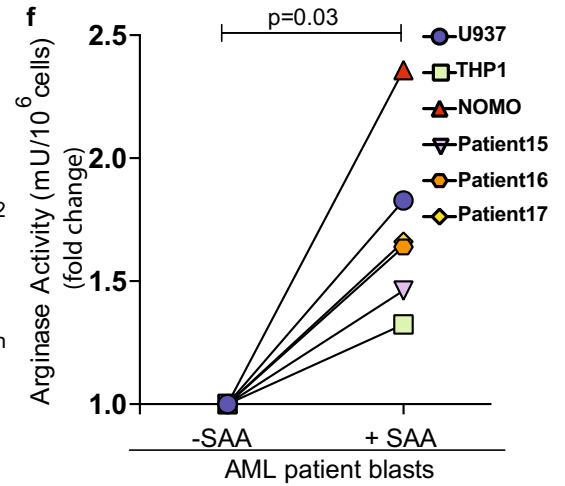
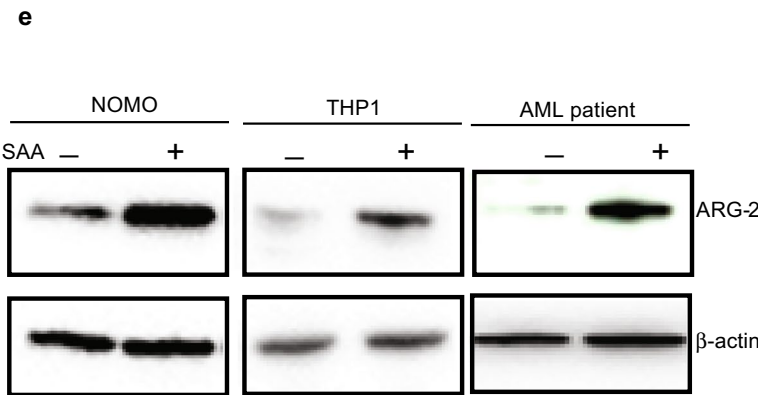
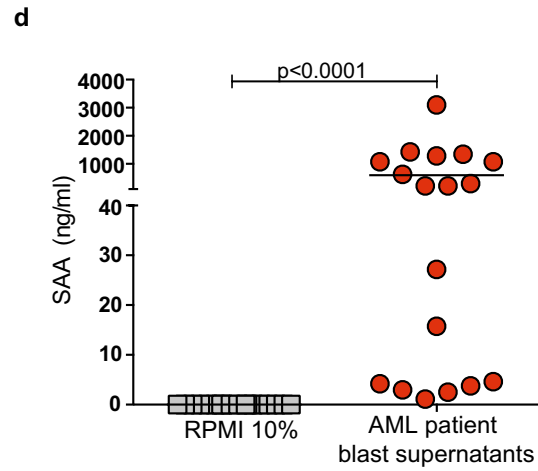
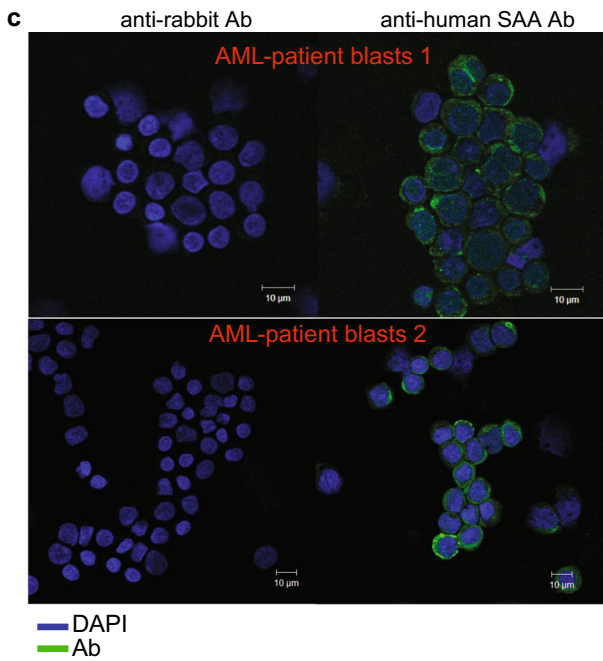
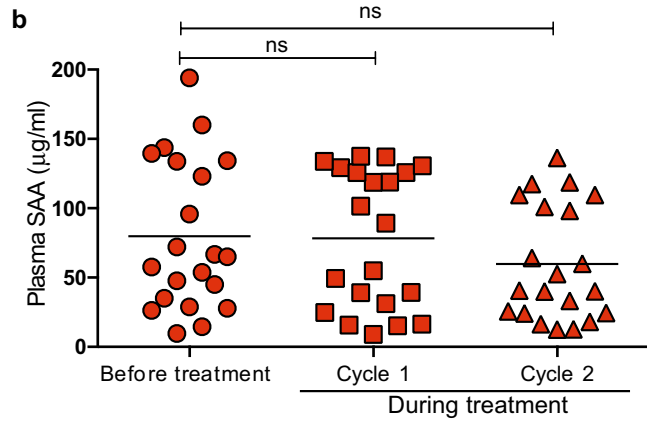
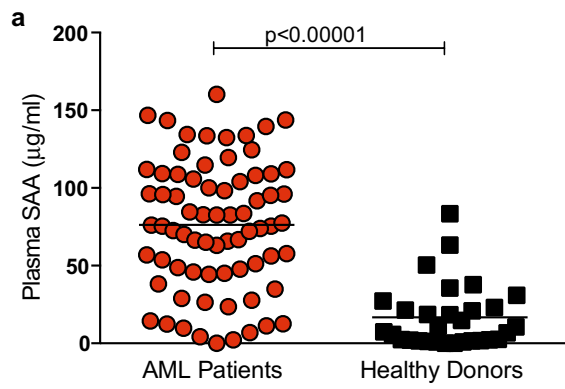


**Fig. 1** SAA upregulates ARG2 in AML blasts. **a** ELISA for SAA in the plasma from  $n=72$  newly diagnosed AML patients prior to treatment, compared to levels in  $n=27$  healthy donors.  $P$  value determined by unpaired  $t$ -test. **b** Plasma SAA concentrations remain unchanged in  $n=20$  AML patients treated with cycles of azacitidine/vorinostat as measured by ELISA.  $P$  value determined by paired  $t$ -test. **c** Confocal microscopy of AML blasts from patients showing intracellular expression of SAA. DAPI—blue, SAA—green, ( $n=2$  individual donors). **d** Increased SAA in the supernatants of AML blasts cultured for 48 h in R10%, measured by ELISA ( $n=18$  patients). Each dot is the mean of duplicates.  $P$  value determined by unpaired  $t$ -test. **e** SAA (10  $\mu\text{g/ml}$ ) leads to upregulation of ARG2 in AML cells, measured by western blot at 72 h. Actin is shown as a loading control. Representative of  $n=3$  individual experiments. **f** Increased arginase activity in AML patients' blasts and cell lines following SAA (10  $\mu\text{g/ml}$ ) treatment for 72 h, as measured by the conversion of arginine into urea. Each dot is the mean of duplicate samples.  $P$  value determined by paired  $t$ -test

The failure of T cell responses against AML blasts is dependent on the interplay of both T cell factors and blast phenotype. T cells from AML patients are reported to demonstrate increased exhaustion, conversion to a Treg phenotype, and failure to generate an immune synapse that leads to activation of cytotoxicity [5, 6]. Concurrently, blasts evade T cell responses through the downregulation of HLA-dependent antigen presentation, expression of inhibitory cell surface molecules, release of immunosuppressive cytokines, and consumption of amino acids critical to T cell expansion [7, 8]. These immunosuppressive strategies are similarly employed by the non-malignant population MDSCs to impair T cell expansion in the setting of solid and haematological cancers [9–11]. Previously, we identified that arginine catabolism by ARG2 contributes to both AML blast viability and suppression of peptide antigen-specific T cell responses in patients [7, 12–14]. ARG2 immunomodulatory activity has since been described in a number of pathological settings, and however, the factors which regulate the enzyme's expression are still poorly understood, including in AML. Inflammatory cytokines may drive malignant transformation or expansion in some AML patients at diagnosis [15].

Although T cells represent a major component of the body's response to cancer, the potential of other immune populations to generate anti-leukaemia immunity or support T cell immunity in solid cancers has not been fully exploited. Here, we investigate how iNKT cells are adapted to the immunosuppression created by AML or MDSCs, resulting in a direct reduction of cancer burden and restoration of T cell function.

## Methods

### Patient samples and study approvals

Blood samples were obtained from 72 AML patients at diagnosis treated at University Hospitals Birmingham and Birmingham Children's Hospital, UK. An additional cohort of samples ( $n=42$ ) was collected from AML patients ineligible for intensive chemotherapy treated with either azacitidine or azacitidine and vorinostat in a multi-centre, randomised phase II trial (RAVVA; NCT01617226) [14]. Fresh peripheral blood mononuclear cells (PBMCs) were separated using a Lymphoprep (StemCell Technologies) gradient and enriched based on CD33 or CD34 expression using anti-human CD33 or anti-human CD34 magnetic beads (Miltenyi) following manufacturer's instructions. All samples were processed in assays within 12 h of blood sampling. Peripheral blood samples from healthy donors were obtained from the University of Birmingham. In accordance with the Declaration of Helsinki, all samples were obtained after written, informed consent prior to inclusion in the study. Regional Ethics Committee (REC Number 10/H0501/39) approval for the study was granted.

### Flow cytometric analysis

Whole blood and PBMCs were stained with human CD1d PBS-57 Tetramer (NIH Tetramer Centre, Emory USA) at 37 °C for 20 min. Following a wash in FACS Buffer, cells were stained for surface antigens: anti-human CD3 (clone UCHT1/HIT3a), CD33 (clone HIM3.4/WM5.3), CD34 (clone 581), FPR2 (clone K102B9), TLR2 (clone TL2.2), TLR4 (clone HTAR5), CD1d (clone 541), CD40 (clone 5C3), CD40L (clone 24–31), FAS (clone DX2), CD69 (clone FN50), CD38 (clone HB-7) antibodies (BioLegend), TCR V $\alpha$ 24 (clone REA948), TCR V $\beta$ 11 (clone REA 559) (Miltenyi Biotec) on ice for 30 min, where indicated. For murine analysis, cells were stained with murine CD1d PBS-57 tetramer (NIH Tetramer Service, USA), SIIN-FEKL tetramer (Biolegend), and anti-murine CD11b (clone M1/70), GR1 (clone 1A8), CD45.1 (clone A20), CD45.2 (clone 104), CD1d (clone 1B1) and CD3 (clone 17A2) (eBiosciences) as indicated. Propidium iodide (PI) (Biolegend) was used to assess viability. Intracellular staining for IFN- $\gamma$  (clone 4S.B3; BioLegend), CD107a (clone H4A3; Biolegend), or ASS1 (Abcam), and goat anti-rabbit IgG (isotype control; Abcam) proteins was determined according to manufacturer's instructions (BioLegend). Where indicated CFSE

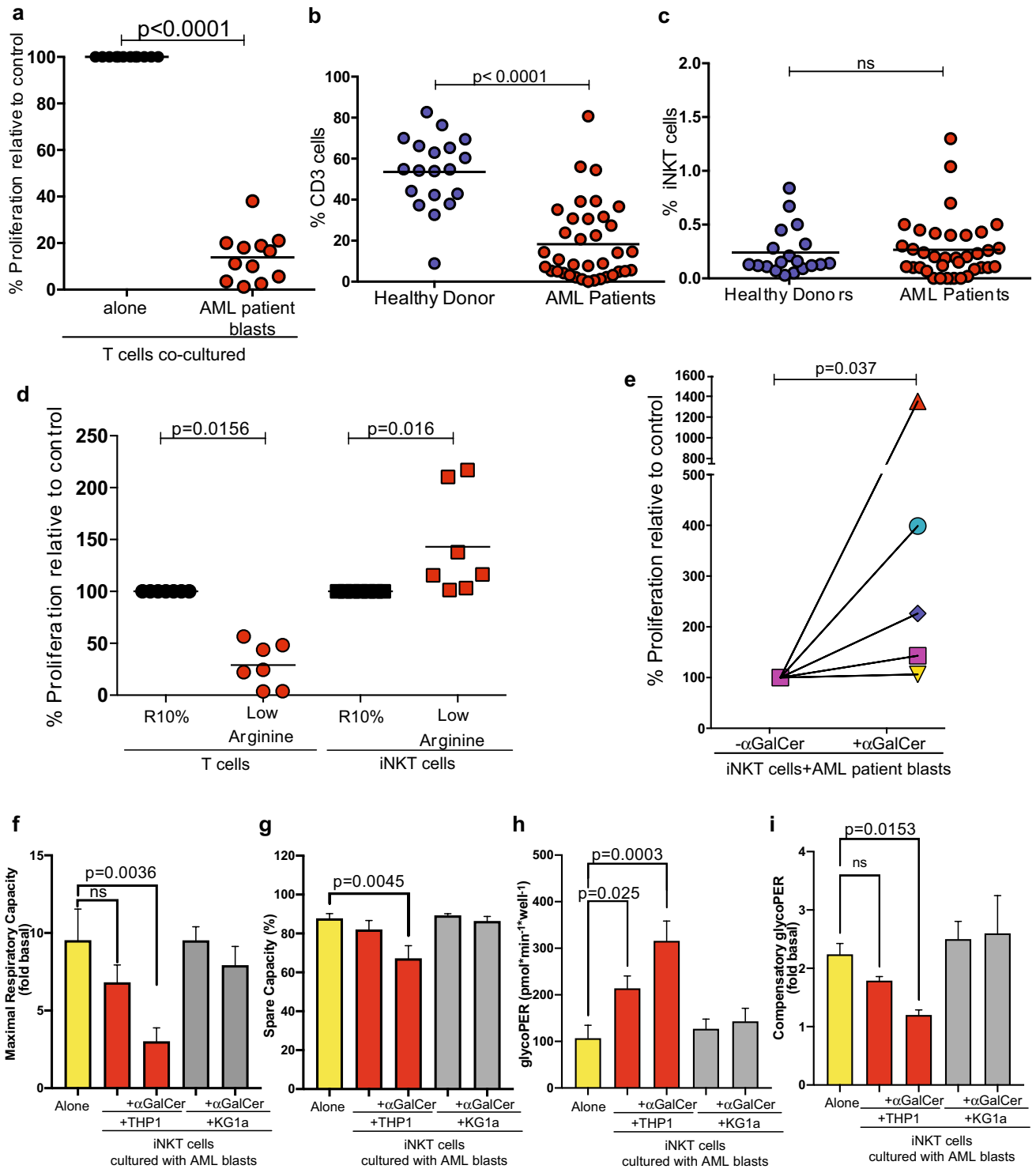


**Fig. 2** iNKT cells are activated following cross-talk with AML blasts. **a** AML blasts suppress T cell proliferation in a mixed leukocyte reaction assay (allogeneic T cells and dendritic cells co-cultured for 96 h).  $n=12$  AML patients. Each dot is the mean of duplicates.  $P$  value determined by paired t-test. **b** The percentage of CD3+ T cells in the blood of healthy donors ( $n=19$ ) and AML patients ( $n=37$ ) at diagnosis measured by flow cytometry.  $P$  value determined by unpaired t-test. **c** The percentage of iNKT cells in the blood of healthy donors ( $n=19$ ) and AML patients ( $n=37$ ) at diagnosis, measured by flow cytometry with CD1d tetramer staining.  $P$  value determined by unpaired t-test. **d** Anti-CD3/anti-CD28 antibody-driven iNKT cell line proliferation ( $n=7$  donors) is unaffected by in vitro culture in low arginine conditions as determined by flow cytometry, after 96 h. Proliferation of T cells ( $n=7$  donors) is suppressed in low arginine. Each dot represents the mean of duplicate samples.  $P$  value determined by paired t-test. **e**  $\alpha$ GalCer (100 ng/ml) presentation by AML blasts induces iNKT cell line proliferation, as measured by flow cytometry after 72 h. Each dot represents the mean of duplicate samples.  $P$  value determined by paired t-test. **f** Mitochondrial oxygen consumption rates (OCR) in the absence and presence of oligomycin were assessed in iNKT cells  $\pm$  THP1 or KG1a  $\pm$   $\alpha$ GalCer (100 ng/ml pulsed for 4 h) to establish maximal respiratory capacity of iNKT cell line, expressed as fold change between BAM 15-induced OCR and baseline OCR. **g** Spare respiratory capacity of iNKT cell lines was calculated as the difference between BAM 15-induced OCR and baseline OCR, expressed as percentage of maximal respiration. Glycolytic proton efflux rates (glycoPER) in the absence and presence of oligomycin were probed in iNKT cell lines to establish baseline rates of glycolysis **h** and compensatory glycolysis (i), respectively. Mitochondrial OCR were corrected for non-mitochondrial respiration by subtracting OCR following rotenone and antimycin addition. GlycoPER were corrected for non-glycolytic acidification by subtracting remaining PER following 2-DG addition. Data are means  $\pm$  SEM from 4 cell donors assessed from two independent microplates each containing 3–4 well replicates per donor. Statistical differences were assessed using one-way ANOVA with Fisher's LSD post hoc test

(Thermo Fisher Scientific) was used to assess AML or iNKT proliferation. CFSE (1:1000 dilution) was added to target cells for 20 min at 37 °C. The assay was quenched with complete media for 5 min, before washing and resuspending. Cells were analysed using a Beckman Coulter Cytotflex flow cytometer and analysed using FlowJo and CytExpert software (Tree Star Inc).

## Murine experiments

Generation of the immortalised MLL-AF9 murine AML cell line has been previously described [14, 16, 17]. MLL-AF9 cells were thawed and resuspended and  $0.5 \times 10^6$  MLL-AF9 cells were transplanted intravenously into sublethally irradiated (4.5 Gy) B6.SJL-Ptprca<sup>a</sup> Pepc<sup>b</sup>/BoyJ (CD45.1+) mice recipients.  $\alpha$ GalCer (2  $\mu$ g/mouse) or vehicle was injected intravenously as indicated in the individual experiments, before the mice were sacrificed at day 17 post-bone marrow

transplant. Serum was collected by tail vein sampling on Day 12. AML donor cells (CD45.2+), iNKT and T cell frequency were identified by flow cytometry of the blood, bone marrow flushed from the legs, and mechanically disrupted spleens following red cell lysis. All vehicle controls were treated with PBS iv.

EG7 lymphoma cells ( $5 \times 10^5$ ) were engrafted subcutaneously into C57BL/6 and iNKT cell-deficient mice ( $J\alpha 18$  TCR gene segment, TCRa  $J^{+m1Tgi}$ ,  $J\alpha 18^{-/-}$ ). Mice were injected with 1  $\mu$ g  $\alpha$ GalCer /mouse following ovalbumin (OVA) vaccine injection ( $10^6$  PFU/mouse) as described previously [18]. Tumour progression, MDSC and OVA-specific T cell expansion were measured. Splenocytes from OT-1 T cell receptor (TCR) transgenic mice ( $5 \times 10^6$ ) were injected into C57BL/6 and  $J\alpha 18^{-/-}$  mice, followed by OVA-peptide (20 ng/ml) pulsed dendritic cells ( $2 \times 10^6$ ). MDSCs were previously isolated by MACS sorting (MDSC Isolation Kit, Miltenyi Biotec) from EG7 tumours engrafted in mice as described above.  $2 \times 10^6$  MDSCs were injected iv followed by  $\alpha$ GalCer (2  $\mu$ g /mouse) where indicated.

Wild-type C57BL/6 mice were treated with 10 mg/kg recombinant human arginase (BCT-100, BCTI, Hong Kong) or PBS iv daily. On day 2, mice were treated with  $\alpha$ GalCer (2  $\mu$ g /mouse) or vehicle iv and all mice were sacrificed on day 5. Blood, bone marrow, and spleens were analysed by flow cytometry as before. Procedures were carried out in accordance with UK Home Office Guidelines.

## Expansion of human iNKT cells

Human iNKT cells were isolated as previously described [18]. In short, PBMCs were isolated from healthy donors' buffy coats by density gradient centrifugation over Lymphoprep<sup>TM</sup> (StemCell Technologies). PBMCs were cultured in complete RPMI, supplemented with  $\beta$ -mercaptoethanol (1X) (SIGMA), in the presence of  $\alpha$ Galactosylceramide ( $\alpha$ GalCer, 100 ng/ml) (BioVision) for 14 days. After 3 days 1000U/ml IL-2 (Novartis) was added to cultures. iNKT cells were isolated by sorting PBMCs labelled with CD1d tetramer (NIH Tetramer service, USA) using a BD FACS Aria Fusion cell sorter. Thereafter, cells were co-cultured with allogenic irradiated PBMCs stimulated with PHA (1  $\mu$ g/ml) (Gibco) and fed every 3–4 days with fresh medium containing 1000 U/ml IL-2 to create 'iNKT cell lines'. iNKT cell frequency was determined using CD1d tetramer (NIH Tetramer Service, Emory USA), V $\alpha$ 24 antibody and V $\beta$ 11 (Miltenyi Biotec). Where indicated primary human iNKT cells were isolated fresh by flow sorting, using human CD1d PBS-57 Tetramer (NIH Tetramer Centre, Emory USA).

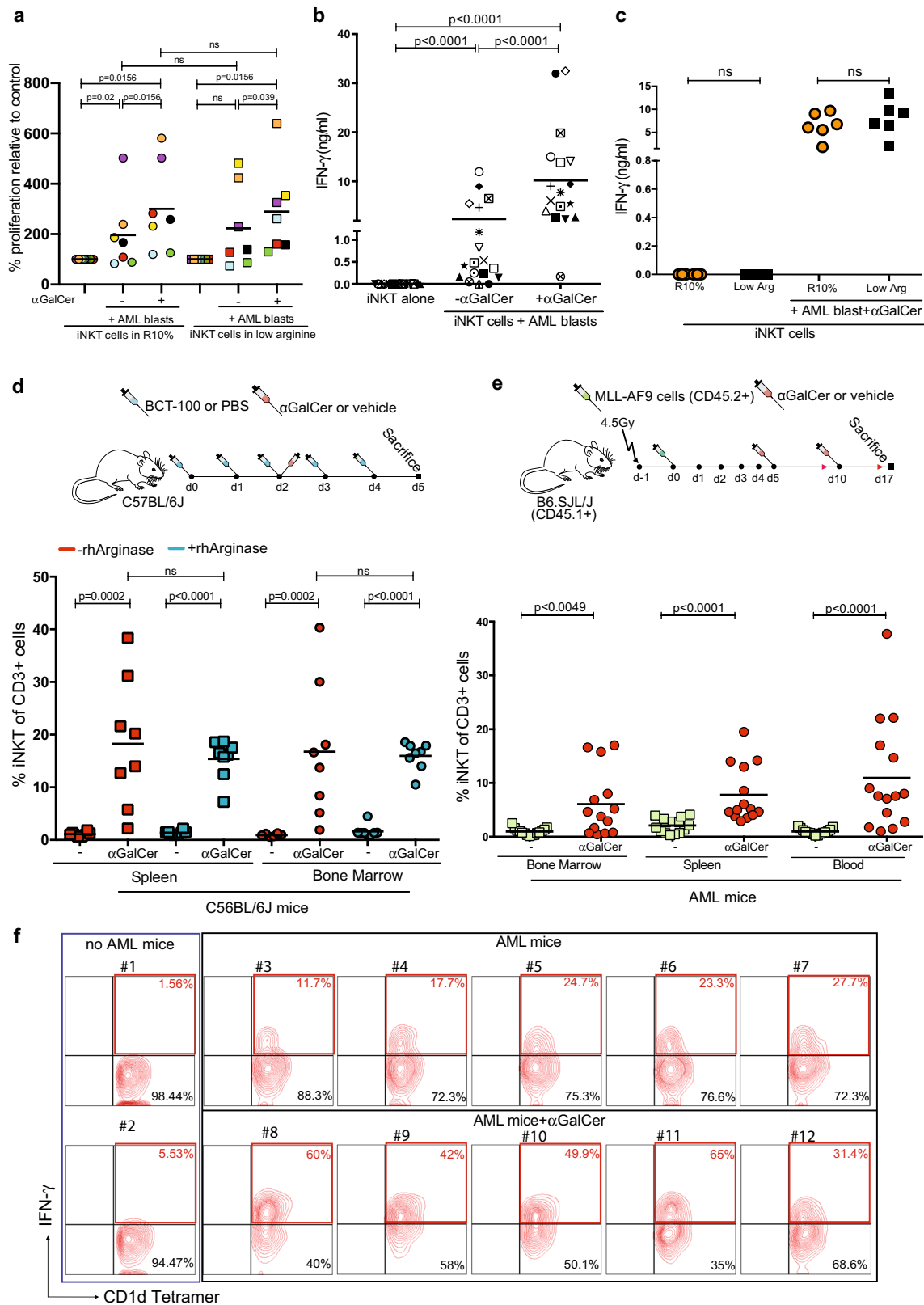


**Fig. 3** iNKT cells remain activated within the low arginine AML environment in vitro and in vivo. **a**  $\alpha$ GalCer (100 ng/ml) presentation by AML blasts induces iNKT cell line proliferation, which is unaffected by low arginine media conditions as measured by flow cytometry after 72 h (blasts from  $n=7$  AML patients). Each dot represents the mean of duplicate samples. *P* value determined by paired t-test. **b** iNKT cell lines cultured with AML blasts for 72 h ( $n=17$  AML patients) in the presence or absence of 100 ng/ml  $\alpha$ GalCer, release IFN- $\gamma$  into culture supernatants as measured by ELISA. Each dot represents the mean of duplicates. *P* value determined by paired t-test. **c**  $\alpha$ GalCer (100 ng/ml) presentation by AML blasts ( $n=6$  AML patients) induces iNKT cell line IFN- $\gamma$  release in vitro after 72 h, which is unaffected by low arginine conditions as measured by ELISA. Representative data of duplicate experiments. *P* value determined by paired t-test. **d** Schematic depicting experimental design. C57BL/6J mice were treated with PBS or recombinant Arginase (BCT-100, 10 mg/kg) in combination with vehicle or 2  $\mu$ g/mouse  $\alpha$ GalCer as indicated. iNKT cell expansion secondary to  $\alpha$ GalCer treatment (iv) is unaffected in C57BL/6J mice ( $n=8$ ) treated with BCT-100 recombinant human Arginase (rhArginase) (iv) as determined by flow cytometry. Representative of two individual experiments. *P* value determined by paired t-test. **e** Schematic depicting experimental design. CD45.1+B6.SJL/J mice were irradiated (4.5 Gy) and engrafted with murine MLL-AF9 AML blasts (CD45.2). Following engraftment mice were treated with vehicle or 2  $\mu$ g/mouse  $\alpha$ GalCer as indicated. iNKT cells (CD1d tetramer positive) proliferate following treatment of MLL-AF9 leukaemia bearing mice ( $n=15$ ) with  $\alpha$ GalCer as measured by flow cytometry. Data from  $n=3$  individual experiments. *P* value determined by unpaired t-test. **f** Flow cytometry plots of iNKT cells from MLL-AF9 leukaemia bearing mice ( $n=14$ ) treated with 2  $\mu$ g/mouse  $\alpha$ GalCer showing upregulation of IFN- $\gamma$  production as measured by intracellular staining. iNKT cells are detected by CD1d tetramer staining. Control mice with no AML or  $\alpha$ GalCer are shown for comparison. Representative data from two individual experiments

### iNKT cell rescue of T cell proliferation assay

T cells were prepared from healthy donors as described above.  $2 \times 10^5$  T cells, enriched by negative selection (Miltenyi Biotec), were cultured with allogenic irradiated (5000 rad) dendritic cells (DC,  $0.5 \times 10^5$ ), in 200 RPMI 5% human serum (Sigma) in 96 well flat bottom plates. Cells were incubated at 37°C, 5% CO<sub>2</sub> for 4 days. 1 mCi/well <sup>3</sup>H-thymidine (PerkinElmer Life Sciences) was added for 12–16 h. <sup>3</sup>H-thymidine incorporation was measured using a Wallac Microbeta Jet 1450 reader (PerkinElmer). AML inhibition of T cell proliferation was carried out by co-culturing AML blasts from patients with healthy donor T cells and irradiated DCs. To test the ability of iNKT cells to overcome AML-induced suppression of T cell proliferation  $0.25 \times 10^5$  iNKT cells were first co-cultured with AML blasts ( $1 \times 10^5$ ) for 8 h, in the presence of  $\alpha$ GalCer (100 ng/ml). After 8 h, the cells were washed and T cells and DC were added to cultures according to the protocol above. Data are expressed

as a percentage of T cell proliferation driven by allogenic irradiated DCs in the presence of AML cells, as compared to allogenic PBMC proliferation in the absence of AML cells (100%). Where indicated iNKT cells were cultured with anti-CD3 (3  $\mu$ g/ml)/anti-CD28 (2  $\mu$ g/ml) in the presence of JPH203 (0.125 mM; J-Pharma, Japan). DMSO was used as a vehicle control.

### iNKT-AML cytotoxicity assay

AML patient blasts and AML cell lines were cultured with iNKT cells and  $\alpha$ GalCer (100 ng/ml) for 24 h, 48 h, and 72 h. Supernatants were harvested to determine cytokine release, and viability of AML blasts was determined by flow cytometry, using propidium iodide (BD Pharmingen) staining.

### Statistics

A Mann–Whitney t-test was used to determine the statistical significance of the difference in unpaired observations between 2 groups (GraphPad Prism, USA). A Wilcoxon matched paired t test was used to determine the statistical significance of the difference in paired observations between 2 groups (GraphPad Prism, USA). *p* values are two-tailed and where values were < 0.05, they were considered statistically significant. For bioenergetic analyses, statistical differences were assessed using one-way ANOVA with Fisher's LSD post hoc test.

## Results

### Serum amyloid A1 (SAA1) upregulates ARG2 in AML blasts

AML blasts induce a low arginine environment in which the immune system must function (Supp Fig. 1a, b). We have previously shown that inflammatory mediators can modulate the phenotype of immunosuppressive myeloid cells, and hypothesised such factors could control ARG2 expression in AML blasts [19]. Evaluation of the plasma of AML patients at diagnosis identified no significant differences in the concentrations of Th1/ Th2 cytokines (Supp Fig. 1c, d). However, SAA levels were significantly raised in AML patients compared to healthy controls (Fig. 1a), and persistent during treatment in a second cohort of patients (Fig. 1b) [14]. Confocal microscopy revealed blasts express SAA (Fig. 1c), which can be released (Fig. 1d) [20, 21].

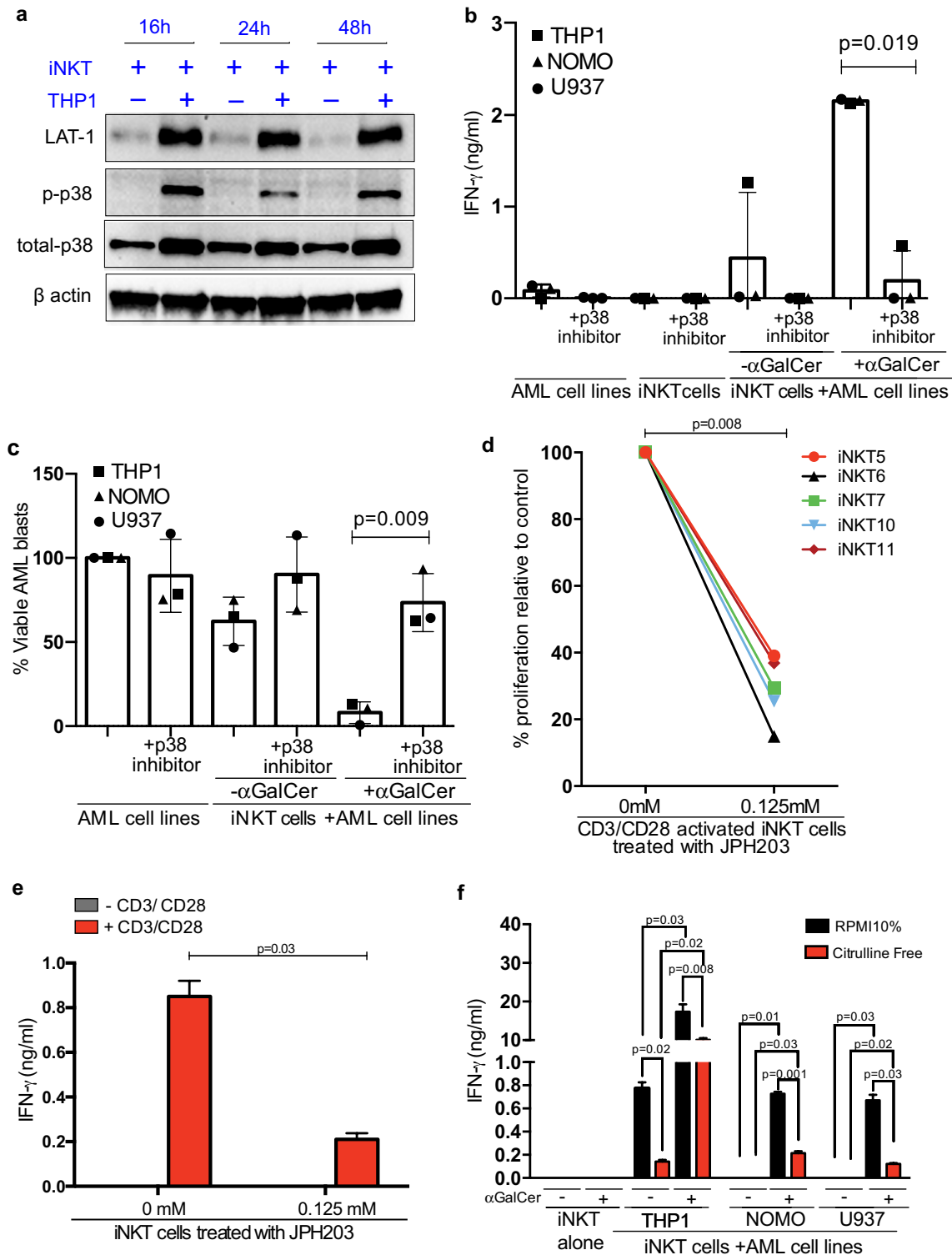


**Fig. 4** iNKT cell proliferation is dependent on citrulline uptake via LAT-1. **a** LAT-1 and p-p38 expression are increased in sorted iNKT cell lines following incubation with AML in the absence of  $\alpha$ GalCer (100 ng/ml) for 72 h. Western blot with actin as a loading control. **b** p38 inhibition (SB203580; 10  $\mu$ M) in iNKT cell lines inhibits IFN- $\gamma$  production after cross-talk with AML cell lines. Each dot is the mean of duplicates. *P* value determined by paired t-test. **c** p38 inhibition (SB203580; 10  $\mu$ M) in iNKT cell lines inhibits cytotoxicity against AML blasts. Each dot is the mean of duplicates. *P* value determined by paired t-test. **d** Primary iNKT cell proliferation (n=5 donors) after 72 h of culture is inhibited by the LAT-1 inhibitor JPH203 (0.125 mM), measured by flow cytometry. Each dot is the mean of duplicates. *P* value determined by paired t-test. **e** LAT-1 inhibition with JPH203 (0.125 mM) impairs primary iNKT activation-induced IFN- $\gamma$  release following stimulation with anti-CD3/CD28 antibodies for 72 h, as measured by ELISA. Each dot is the mean of duplicates. *P* value determined by paired t-test. **f** iNKT  $\alpha$ GalCer (100 ng/ml) cell line activation-induced IFN- $\gamma$  release is inhibited in the absence of citrulline, in co-cultures with AML cell lines for 72 h. *P* value determined by paired t-test

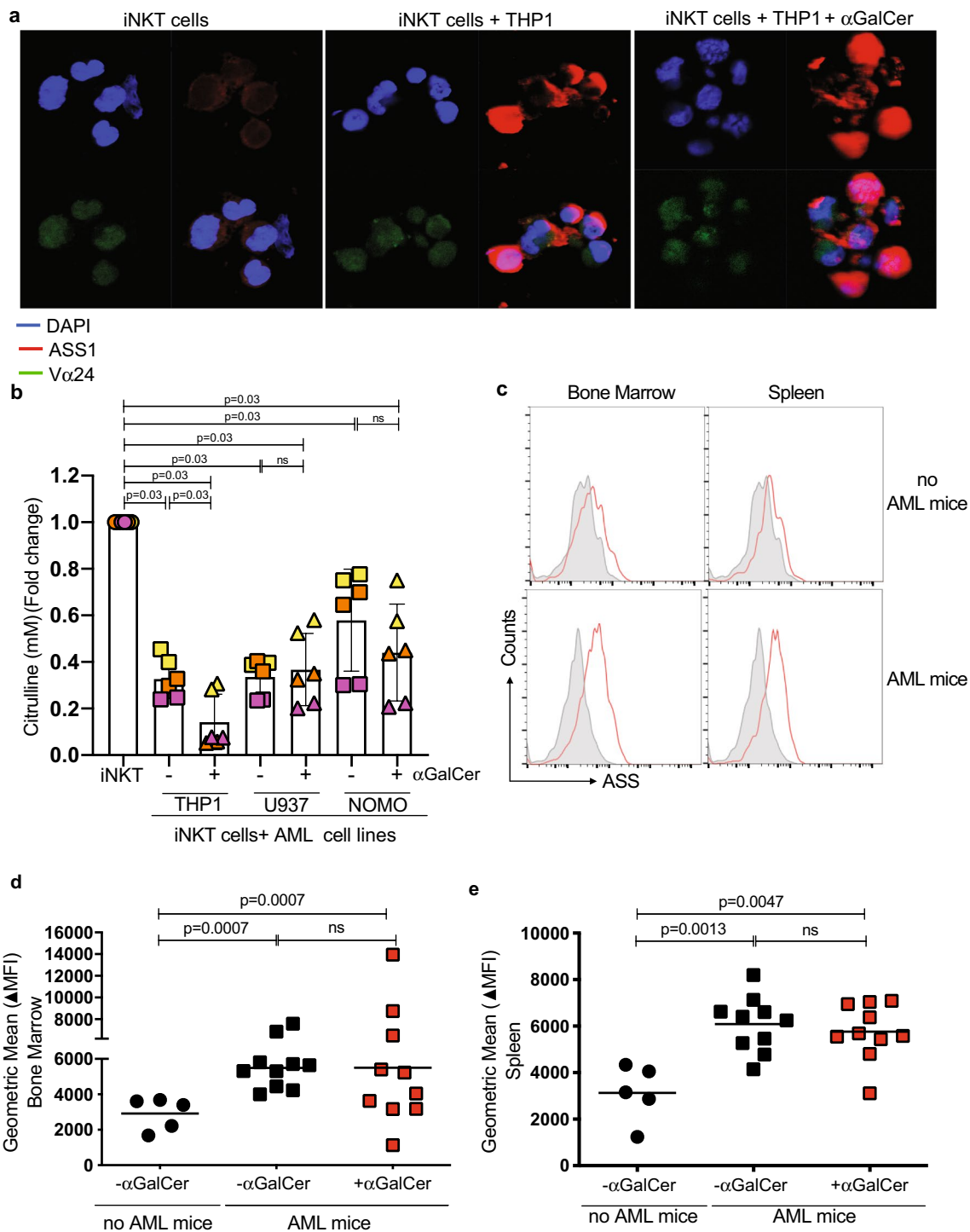


**Fig. 5** ASS catalyzes citrulline in iNKT Cells. **a** Confocal microscopy of primary sorted iNKT cells showing increased ASS1 expression following crosstalk with THP-1 cells for 72 h. DAPI—blue, ASS-1—red, and V $\alpha$ 24—green. **b** iNKT cell lines have increased ASS1 enzyme activity, following cross-talk with AML blasts for 72 h. ASS1 enzyme activity of sorted iNKT cells lysates was determined by citrulline depletion using a colorimetric assay. Data from  $n=3$  individual experiments.  $P$  value determined by paired t-test. **c** Representative flow cytometry histograms of iNKT cells sorted from the bone marrow and spleens of  $n=10$  MLL-AF9 leukaemia bearing mice, demonstrating ASS expression as measured by intracellular

staining. Data from  $n=2$  individual experiments. **d** Geometric means for ASS intracellular staining of iNKT cells sorted from the bone marrow of  $n=10$  MLL-AF9 leukaemia bearing mice, demonstrating increased ASS expression compared to non-leukaemia control mice in the presence or absence of 2  $\mu$ g /mouse  $\alpha$ GalCer. Data from  $n=2$  individual experiments.  $P$  value determined by unpaired t-test. **e** Geometric means for ASS intracellular staining of iNKT cells sorted from the spleens of  $n=10$  MLL-AF9 leukaemia bearing mice, demonstrating ASS expression compared to non-leukaemia control mice in the presence or absence of 2  $\mu$ g /mouse  $\alpha$ GalCer. Data from  $n=2$  individual experiments.  $P$  value determined by unpaired t-test

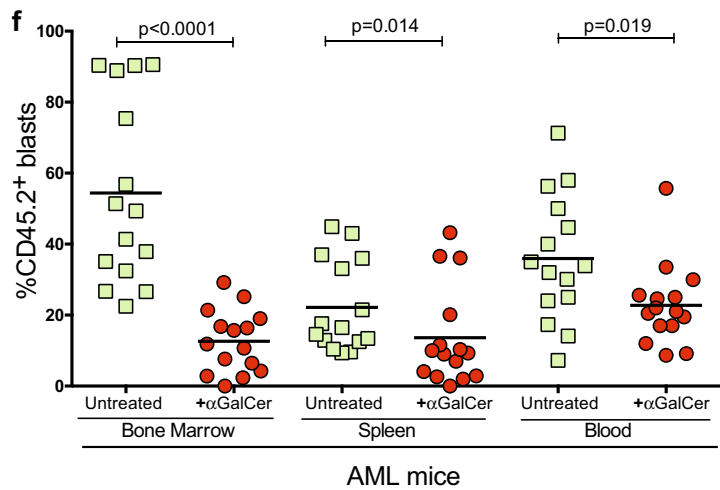
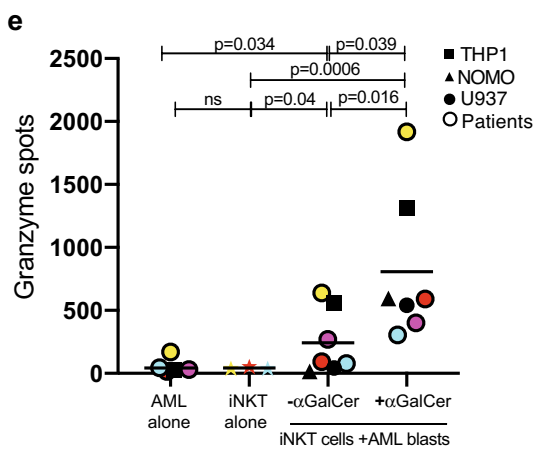
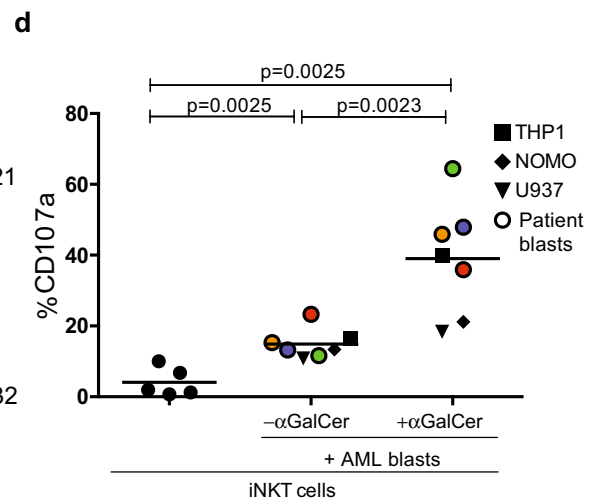
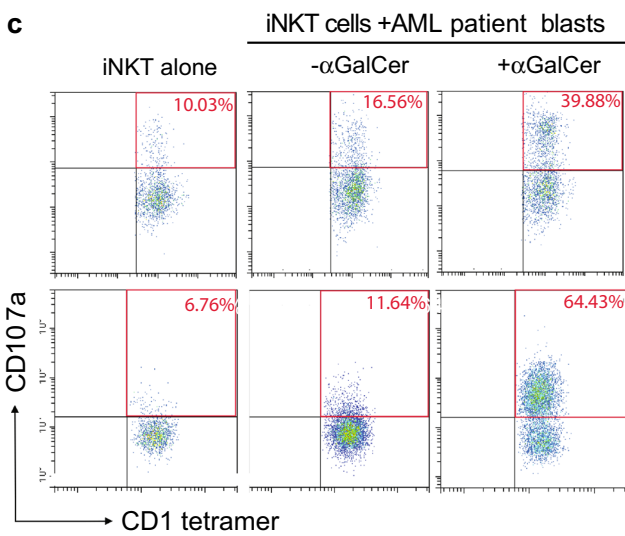
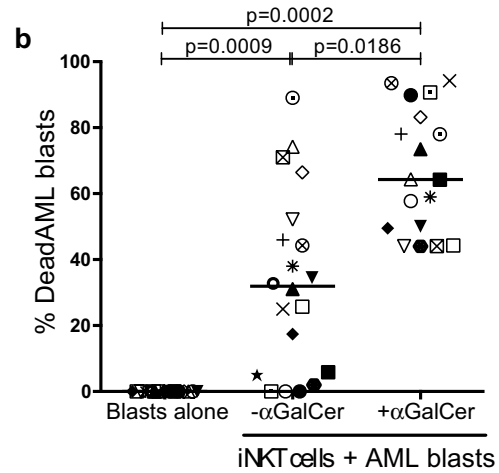
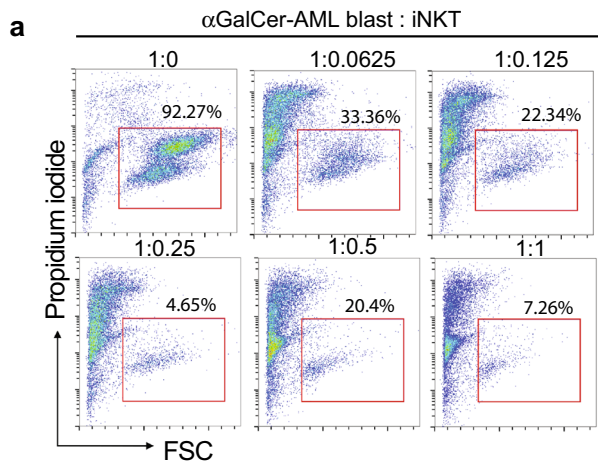


**Fig. 6** iNKT cell activation induces AML cell death. **a**  $\alpha$ GalCer (100 ng/ml) enhances iNKT cell line cytotoxicity against AML blasts after 72 h of culture. Representative flow cytometry of  $n=18$  patients, gated on propidium iodide staining versus forward scatter (FSC) of AML blasts. **b** Pooled analysis demonstrating  $\alpha$ GalCer (100 ng/ml) enhances iNKT cell line cytotoxicity against AML blasts ( $n=18$  donors) as measured by flow cytometry. (1iNKT:4AML blasts).  $P$  value determined by paired  $t$ -test. **c** Representative flow cytometry of iNKT cells, gating on CD1d tetramer versus CD107a, after iNKT co-culture with AML blasts. Two representative patients of  $n=7$  total. **d** iNKT cells undergo degranulation, exemplified by CD107a upregulation, following  $\alpha$ GalCer (100 ng/ml) induced cross-talk with AML ( $n=3$  cell lines and  $n=4$  AML patient samples) for 72 h. Each dot is the mean of duplicates. **e** Increased granzyme B expression in iNKT cell lines after 72 h of cross-talk with  $n=3$  AML cell lines and  $n=3$  AML patients as measured by ELISPOT. Each dot is the mean of duplicates. **f** iNKT cell activation with  $\alpha$ GalCer (2  $\mu$ g / mouse on days 5 and 10 *iv*) in vivo leads to a reduction in MLL-AF9 leukaemia burden in the bone marrow, spleen, and blood ( $n=15$  mice untreated mice and  $n=15$  mice treated with  $\alpha$ GalCer). AML blasts (CD45.2) were measured by flow cytometry. Data from  $n=3$  individual experiments.  $P$  value determined by unpaired  $t$ -test

AML blasts were treated with recombinant SAA, leading to an increase in blast viability *ex vivo* (Supp Fig. e, f). Evaluation of cell lines and patients' blasts identified expression of the SAA receptors Toll-like Receptors: TLR2, TLR4, and Formyl-Peptide Receptor 2 (FPR2) (Supp Fig. 2a). Sequential blockade reveals SAA signals through FPR2 (Supp Fig. 2b, c), contributing to local inflammation by increasing the production and release of IL-1 $\beta$  (Supp Fig. 2d, e). Notably, SAA leads to the upregulation of intracellular ARG2 expression and activity (Fig. 1e, f), and a corresponding reduction in extracellular arginine (Supp Fig. 2f).

### iNKT cells are adapted to the low arginine microenvironment through LAT-1 and ASS1 expression

The failure of immune surveillance contributes to leukaemia progression. Although we and others have shown that T cells numbers are suppressed in the low arginine AML niche *ex vivo* (Fig. 2a), and in patients (Fig. 2b), we observe that the specialised population of invariant natural killer T cells (iNKT) remains unchanged (Fig. 2c, Supp Fig. 3a) [7]. To investigate the capacity of iNKT to respond in low arginine conditions, sorted cells were stimulated using anti-CD3/anti-CD28 antibodies (Supp Fig. 3b). Although iNKT cells proliferated under low arginine, conventional T cell proliferation was suppressed (Fig. 2d).

iNKT cells recognise glycolipid antigens presented by myeloid cells via the MHC-like molecule CD1d in combination with CD40 co-stimulation. Flow cytometry identified CD1d and CD40 are expressed on patients' blasts (Supp

Fig. 3c, d). Next, we investigated antigen-specific iNKT proliferation by AML under stimulation with  $\alpha$ GalCer, a synthetic glycolipid that is an established activator of iNKT cells used in experimental models and clinical trials [22]. Antigen-induced iNKT proliferation was unaffected by AML conditions (Fig. 2e, Supp Fig. 3e). Oxidative and glycolytic flux of iNKT cells was probed using an Agilent Seahorse XFe96 Analyzer. Despite modest differences, neither basal mitochondrial nor ADP phosphorylation-linked respiration were significantly altered between iNKT cells and those co-cultured with AML  $\pm$   $\alpha$ GalCer (Supp Fig. 3f–i). However, crosstalk of iNKT cells with AML significantly lowered maximal mitochondrial respiratory capacity of iNKT cells from 9.5-fold of basal to threefold of basal when treated with  $\alpha$ GalCer (Fig. 2f). Spare respiratory capacity was also significantly lower (Fig. 2g). No significant differences were observed on either maximal respiratory capacity or spare respiratory capacity in iNKT cells co-cultured with the CD1d negative line KG1a  $\pm$   $\alpha$ GalCer (Fig. 2f, g). Glycolytic Proton Efflux Rate (GlycoPER) was significantly increased in iNKT cells after AML crosstalk (Fig. 2h), and oligomycin-induced compensatory glycoPER is lower in iNKT cells after crosstalk with THP1 but not KG1a  $\pm$   $\alpha$ GalCer (Fig. 2i). Consistent with this, rates of ATP synthesis linked to glycolysis were significantly increased in iNKT cells after THP1 co-culture  $\pm$   $\alpha$ GalCer when compared to iNKT cells alone or those co-cultured with KG1a  $\pm$   $\alpha$ GalCer (Supp Fig. 3j). These data suggest a dependence on glycolytic flux to meet cellular ATP demand in the early phase of activation in iNKT cells. Notably, the lower spare respiratory capacity and increased glycolytic rates of ATP synthesis observed after iNKT cells are cultured with CD1d + AML are consistent with the metabolic changes that occur upon naïve T cell activation [23, 24].

Functional evidence for the above activation findings was confirmed. Stimulation of iNKT proliferation by AML with  $\alpha$ GalCer was unaffected, even under lower arginine conditions *in vitro* (Fig. 3a). Culture of iNKT with AML blasts leads to activation-induced IFN- $\gamma$  production and release (Supp Figs. 4a, 3b), which is also unaffected by low arginine media conditions *in vitro* (Fig. 3c). Increased levels of the activation markers CD69, CD38 and FAS are similarly observed in both conditions (Supp Fig. 4b, c).

To support these findings immunocompetent mice were depleted of arginine using recombinant arginase (Supp Fig. 4d). *In vivo* iNKT cells retained the capacity to expand (Fig. 3d, Supp Fig. 4e) and release IFN- $\gamma$  (Supp Fig. 4f) on  $\alpha$ GalCer antigen stimulation. In an immunocompetent AML murine model (MLL-AF9) that replicated a low arginine environment (Supp Fig. 1b), we similarly demonstrate iNKT

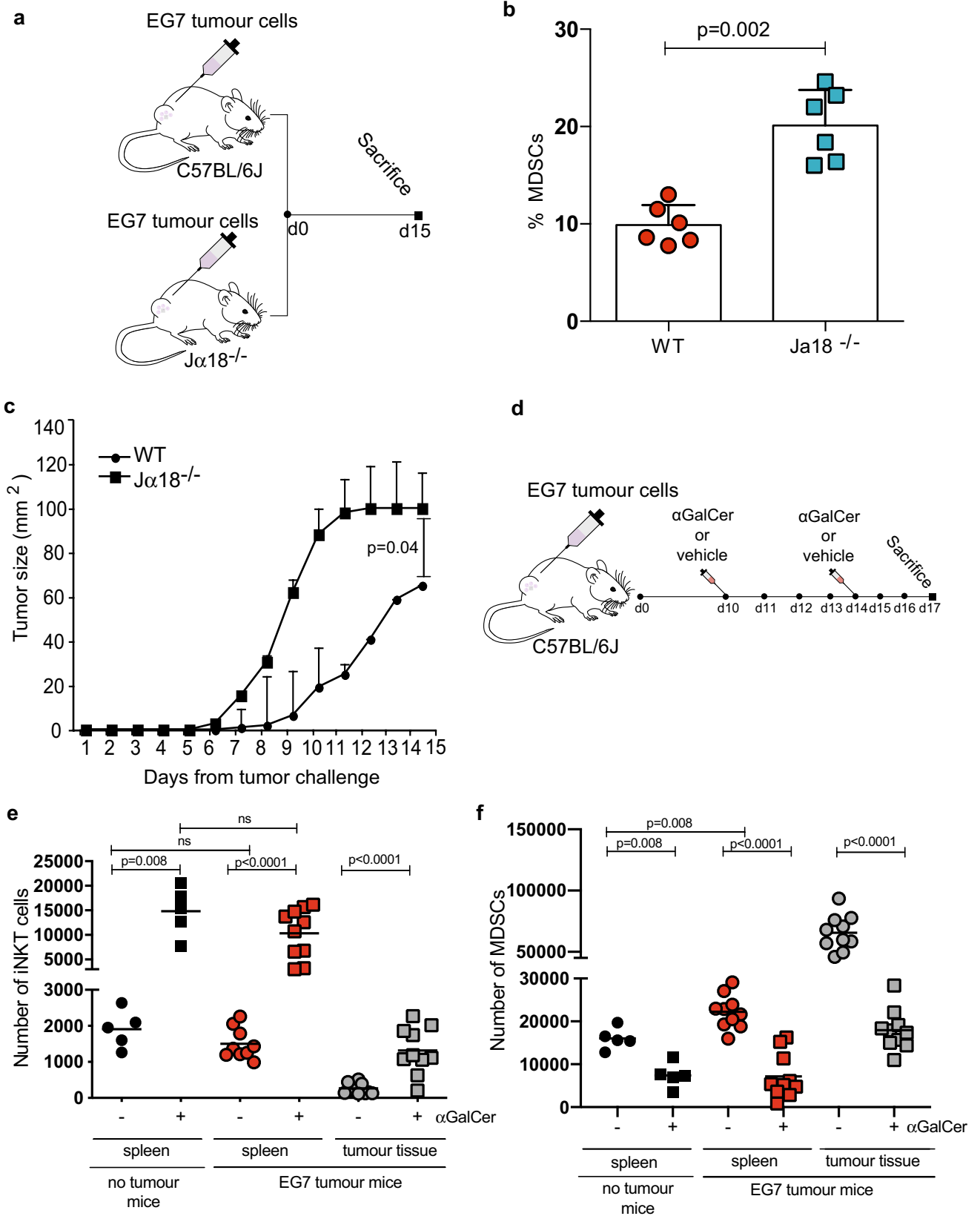


**Fig. 7** iNKT cells control MDSC numbers in an EG7 lymphoma model. **a** Schematic depicting experimental design. C57BL/6J or  $J\alpha 18^{-/-}$  mice were engrafted with EG7 cells subcutaneously. 15 days later mice were sacrificed. **b** MDSCs are increased in the spleens of  $J\alpha 18^{-/-}$  mice ( $n=6$ ) compared to wild-type (WT;  $n=6$ ), as measured by flow cytometry.  $P$  value determined by unpaired t-test. **c** Lymphoma (EG7) growth is faster in ( $n=6$ )  $J\alpha 18^{-/-}$  mice compared to wildtype (WT; ( $n=6$ ).  $P$  value determined by unpaired t-test. **d** Schematic depicting experimental design. C57BL/6J were engrafted with EG7 cells subcutaneously. Mice were treated with iv  $\alpha$ GalCer 2  $\mu$ g /mouse or vehicle on days 10 and 14, before being sacrificed on day 17. **e** iNKT cells expand in the tumours and spleens of EG7 lymphoma-bearing following  $\alpha$ GalCer ( $n=10$  mice per group, vs  $n=5$  no tumour-bearing mice controls). Data of two individual experiments.  $P$  value determined by unpaired t-test. **f** MDSCs are reduced in the tumours and spleens of EG7 lymphoma-bearing mice following  $\alpha$ GalCer 2  $\mu$ g /mouse ( $n=10$  mice per group, vs  $n=5$  no tumour-bearing mice controls). Data two individual experiments.  $P$  value determined by unpaired t-test

cells proliferate in bone marrow, spleen, and blood environments of AML-bearing mice (Fig. 3e) [14, 17]. Activated iNKT within the bone marrow produce and release IFN- $\gamma$  (Fig. 3f, Sup Fig. 4g, h).

We hypothesised that the iNKT cells may be adapted to low arginine environments by switching away from arginine metabolism. Sorted iNKT cells activated in low arginine conditions were subject to ultra-high performance liquid chromatography mass spectrometry (UHPLC-MS) analysis and demonstrated metabolic perturbations in the arginine and proline metabolism pathway as expected. Pathway enrichment analysis revealed changes in *valine, leucine and isoleucine biosynthesis, glycine, serine and threonine metabolism, alanine, aspartate and glutamate metabolism, and cysteine and methionine metabolism*. (Supplementary Table 1) Consistent with this, isolated iNKT cells post-cross-talk with AML cell lines have upregulation of the transmembrane amino acid transporter LAT-1 (SLC7A5) which mediates uptake of neutral amino acids (Fig. 4a) [25]. LAT1 upregulation is increased with accompanying p38 phosphorylation (Fig. 4a). Inhibition of p38 phosphorylation abrogates iNKT IFN- $\gamma$  release and cytotoxicity (Fig. 4b, c). Inhibition of LAT-1 with the small molecule inhibitor JPH-203 impairs human iNKT proliferation (Fig. 4d), and IFN- $\gamma$  release (Fig. 4e), with no effect on viability (Supp Fig. 4i).

Complimentary to data shown in Fig. 2, iNKT cells in the presence of citrulline exposed to THP1  $\pm$   $\alpha$ GalCer present significant metabolic changes as measured by Seahorse assay (Supp Fig. 5a–h). The absence of citrulline also impairs antigen-induced IFN- $\gamma$  release (Fig. 4f). Citrulline is transported by LAT-1 and catabolised by ASS1, an enzyme

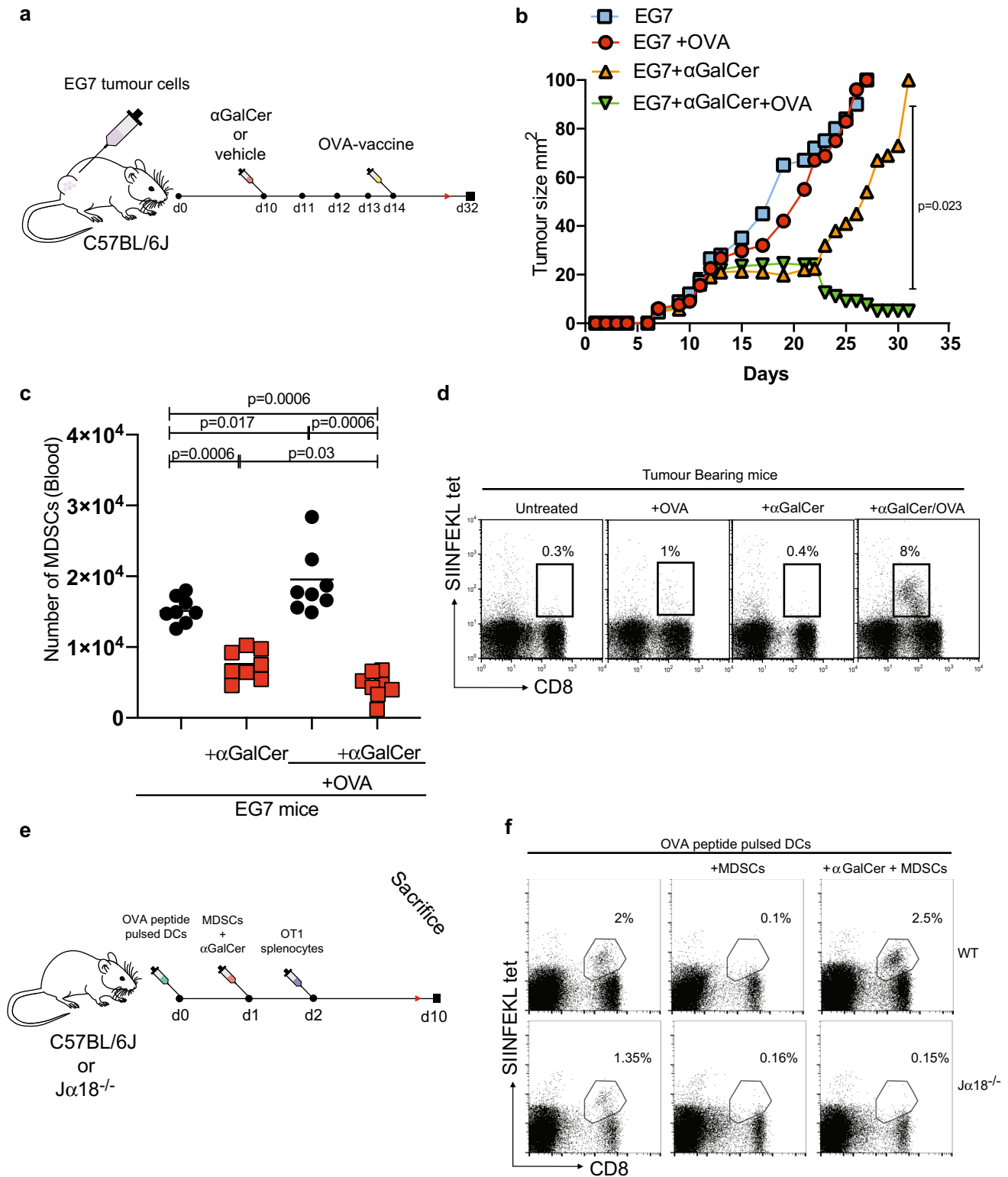
which infers resistance to a low arginine microenvironment (Supp Fig. 5g). After cross-talk with CD1d + AML (THP-1), ASS1 expression is upregulated in freshly isolated iNKT cells (Fig. 5a, and Supp Fig. 5h–j) with concurrent increased enzyme activity (Fig. 5b). Minimal change in the expression of other enzymes within the arginine metabolism pathway was seen (Arginase 1—ARG1, ARG2, Ornithine Transcarbamylase—OTC, Argininosuccinate Lyase—ASL) (Supp Fig. 5k). Confirming these findings ASS1 enzyme expression is similarly increased in murine iNKT cells within the AML environment in vivo (Fig. 5c–e).

### CD1d-iTCR-dependent cross-talk induces AML apoptosis

Having demonstrated that iNKT cells are functional in the AML niche we investigated the impact of iNKT cells on AML disease burden. iNKT cells are cytotoxic to blasts on antigen presentation (Fig. 6a, b, Supp Fig. 6a) in a CD1d-CD40-dependent manner (Supp Fig. 6b, c). Blockade of CD1d prevents IFN- $\gamma$  release (Supp Fig. 6d). iNKT cells undergo degranulation exemplified by CD107a upregulation (Fig. 6c and d), and granzyme release (Fig. 6e). The result is induction of AML blast apoptosis characterised by Caspases 9,3 and PARP cleavage (Supp Fig. 6e, Supp Fig. 7a). In vivo activation of iNKT cells with  $\alpha$ GalCer similarly leads to a significant reduction in CD1d + AML (Supp Fig. 7b) burden in the blood, spleen, and bone marrow (Schematic Figs. 3e and 6f).

### iNKT rescue antigen-specific T cell proliferation in other myeloid-derived immunosuppressive microenvironments

Physiological antigen-specific conventional T cell expansion in AML patients or patients with solid cancers is often incapable of controlling cancer progression. Clinical trials of T cell therapies remain suboptimal outside of B-cell malignancies, due to poor T cell persistence and activation and the impact of MDSCs [26, 27]. As we show that iNKT cells can function within a low arginine microenvironment we investigated their role as an adjunct to T cell immunotherapy in two further models. Co-culture of allo-antigen-driven T cells with AML blasts led to a reduction in T cell proliferation, which was restored in the presence of activated iNKT



cells (Supp Fig. 7c). These findings are recapitulated *in vivo* with AML-bearing mice (MLL-AF9) similarly undergoing a rescue of T cell frequency in the spleen and bone marrow after αGalCer treatment (Supp Fig. 7d).

MDSCs and AML blasts share phenotypic and immunosuppressive similarities [9–11]. Therefore, we investigated the function of iNKT in a second immunocompetent system, using a syngeneic lymphoma model that induces CD11d positive MDSCs *in vivo* (Supp Fig. 7e, f). EG7 lymphoma

**Fig. 8** iNKT cells control MDSC numbers in an EG7 lymphoma model. **a** Schematic depicting experimental design. C57Bl/6J mice were engrafted with EG7 cells subcutaneously. Mice were treated with iv  $\alpha$ GalCer 2  $\mu$ g/mouse or vehicle on day 10. Two groups were treated with OVA-vaccine on day 14. **b** Lymphoma (EG7) growth is inhibited in OT-1 mice treated with OVA and 2  $\mu$ g/mouse  $\alpha$ GalCer ( $n=8$  mice per group). *P* value determined by unpaired t-test. **c** EG7 lymphoma-bearing mice (C57Bl/6J), treated with OVA-vaccine and 2  $\mu$ g/mouse  $\alpha$ GalCer ( $n=8$  mice per group), have a corresponding decrease in the total number of MDSCs in the blood. *P* value determined by unpaired t-test. **d** Representative flow cytometry plot, gated on CD8 versus SIINFEKL-tetramer positive T cells, demonstrating increased SIINFEKL antigen-specific T cells in the blood of EG7 lymphoma-bearing mice ( $n=8$ ) treated with OVA-vaccine and 2  $\mu$ g/mouse  $\alpha$ GalCer. **e** Schematic depicting experimental design. C57Bl/6J or  $J\alpha 18^{-/-}$  mice were administered OVA-peptide-loaded dendritic cells (DC) and adoptively transferred tumour-derived MDSCs. Following the administration of  $\alpha$ GalCer (2  $\mu$ g/mouse) and OT1 splenocytes iv mice were sacrificed on day 10. **f** Antigen-specific T cells expansion is inhibited by the lack of iNKT cells in  $J\alpha 18^{-/-}$  mice adoptively transferred with tumour-derived MDSCs. Representative flow cytometry gating of SIINFEKL tetramer labelled T cells from the spleens. Representative data of two individual experiments

cells were engrafted into wild-type and iNKT cell-deficient mice ( $J\alpha 18^{-/-}$  mice) (Fig. 7a).  $J\alpha 18^{-/-}$  mice have a relative increase in MDSCs (Fig. 7b) and developed larger tumours (Fig. 7c) compared to WT mice. To evaluate the potential role of iNKT activation in MDSC control, EG7 tumour-bearing mice were treated with  $\alpha$ GalCer (Fig. 7d) leading to an increase in iNKT cell frequency in the tumours and spleens (Fig. 7e), and associated IFN- $\gamma$  release into the serum (Supp Fig. 7g), with a reduction in the MDSCs in these tissues (Fig. 7f). We confirmed iNKT cells within the EG7 tumour microenvironment express ASS1, regardless of  $\alpha$ GalCer treatment (Supp Fig. 8a, b).

Next to evaluate the impact of iNKT activation on conventional T cell immunity, antigen-specific T cells were induced with OVA-peptide vaccine (Fig. 8a). Vaccine alone led to no significant control of tumour growth (Fig. 8b). However, combination with  $\alpha$ GalCer led to a significant slowing of tumour growth (Fig. 8b), reduction of MDSC frequency in blood (Fig. 8c) and an enhanced OVA-specific T cell proliferation (Fig. 8d and Supp Fig. 8c).

To confirm the capacity of activated iNKT to overcome MDSC inhibition of conventional T cells, MDSCs from EG7 lymphoma-bearing mice were adoptively transferred into wild-type (WT) and  $J\alpha 18^{-/-}$  naïve mice (Fig. 8e). MDSCs abolished in vivo expansion of adoptively transferred OT-I splenocytes following peptide priming (Fig. 8f and Supp Fig. 8d). In contrast, when the transfer of MDSCs was followed by an injection of  $\alpha$ GalCer in  $J\alpha 18^{-/-}$  mice, no expansion of adoptively transferred OT-I cells was observed (Fig. 8f, Supp Fig. 8d).

## Discussion

We demonstrated that iNKT cells function within the immunosuppressive environments created by AML or MDSCs to reduce myeloid numbers and enhance antigen-specific T cell responses. AML and MDSCs share a number of characteristics, not least their myeloid origin, but also the downregulation of HLA-DR and suppression of T cell proliferation. One of the most well-characterised suppressive mediators in MDSCs is the expression of ARG1, which catabolises arginine to deprive T cells [28, 29]. The regulation of ARG1 expression in MDSCs by IL-4, HIF-1 $\alpha$ , and STAT3 is well established; however, the factors which regulate ARG2 in tumour cells have received less attention to date [30, 31]. Here, we show that serum amyloid A is produced by AML blasts and promotes blast viability through FPR2. Notably, SAA also regulates IDO expression in AML blasts [32]. SAA has been reported to regulate ARG1 and ARG2 in endothelial cells or macrophages, which may promote myeloid cell survival during infection and inflammation [33–35]

Previously, we and others have shown that although T cells can recognise a number of peptide antigens presented by AML blasts in the context of HLA molecules, the capacity to meaningfully boost these responses in clinical trials is challenging [14, 36]. The identification that CD1d is expressed on AML blasts provides an opportunity to use non-peptide-based strategies to target AML. The number of iNKT cells in different cohorts of AML patients may vary [37, 38]. The role of iNKT cells as critical to anti-leukaemia immune surveillance was highlighted in a study demonstrating that the failure of iNKT cells to reconstitute in AML patients post-T cell-depleted HLA-haploidentical haematopoietic stem cell transplant (HSCT) correlated with relapse [39]. To date no clinical trials of iNKT cells against AML have taken place. The use of exogenous glycolipids, namely  $\alpha$ GalCer, has the potential to translate our findings for therapeutic benefit.  $\alpha$ GalCer remains an attractive therapeutic as it is relatively cheap to synthesise and has already completed Phase I and II clinical trials in adult solid tumours, demonstrating an excellent safety profile. We have shown  $\alpha$ GalCer is capable to induce a number of critical effects including an increase of iNKT numbers, activation-induced IFN- $\gamma$  release, a direct iNKT-derived cytotoxicity against AML blasts in vivo, and restoration of T cell function—expanding the rationale from previous in vitro reports [40, 41]. Interestingly, the potential of  $\alpha$ GalCer-induced iNKT cell expansion has been harnessed in a hybrid fashion through the preclinical development of anti-CD19 iNKT CAR-T cells for lymphoma [42]. As AML blasts can directly present  $\alpha$ GalCer to iNKT cells, the need for a loaded-dendritic cell vaccine or allogeneic approaches is

also circumvented making the drug readily deliverable even to fragile AML populations such as children and the elderly.

We find that iNKT cells can function within the low arginine conditions created by AML, that is hostile to T cells. Although T cells require arginine for proliferation and activation, we show that iNKT cells do not express the cellular machinery for arginine catabolism (Arginase 1 or Arginase 2) but instead upregulate amino acid uptake via SLC7A5 (LAT-1) which feed forward into the ASS1 pathway. The binding partner of SLC transporters, CD98, has previously been reported on murine iNKT cells [43]. These findings help explain how iNKT cells can also function to abolish ARG1 + MDSCs that suppress T cells in the setting of influenza [44]. As such iNKT cells have a seemingly unique adaptation to the amino acid metabolic microenvironment of tumours, identifying a new niche functionality for these relatively rare immune cells. We highlight that  $\alpha$ GalCer activation of iNKT cells leads to a secondary enhancement of antigen-specific T cell immunity not only in AML but in solid cancer—a hitherto unutilised finding. Although as a single agent  $\alpha$ GalCer-iNKT responses against solid tumours in clinical trials have been disappointing, our data suggest a better strategy is to combine  $\alpha$ GalCer-induced iNKT activation as an adjuvant to T cell immunotherapies. We show that iNKT activation abrogates the expansion and immunosuppressive activity of tumour-associated MDSCs in immunocompetent murine models and allows antigen-specific T cells to eradicate tumour burden. In many respects, this mimics the multi-cellular immunological response that is physiologically generated on immune activation against foreign pathogens [45]. Targeting of MDSCs remains a major challenge in the era of cellular immunotherapy, due to the heterogeneity of MDSC phenotype both within patients and across diseases. Although MDSC depletion with cytotoxic chemotherapy remains an approach used prior to CAR-T/adoptive T cell administration, the short-lived effectiveness of such an approach likely contributes to the failure of T cell therapies in solid cancers [46]. As iNKT cells are produced endogenously by patients and circulate both through the blood and tumour compartments, iNKT cells could be activated in patients by treatment with  $\alpha$ GalCer or ex vivo using apheresed and expanded products. Thus, iNKT cell therapy could be given alongside other immune therapies, such as CAR-T, and provide a sustainable, translatable and low toxicity approach to enhance immunotherapy.

## Key points

iNKT cells cross-talk with AML blasts via CD1d-dependent signalling, resulting in AML apoptosis and reduction of leukaemic burden in vivo. iNKT upregulate LAT-1/ ASS1 in

low arginine environments leading to activation of antigen-specific T cells and tumour clearance.

**Supplementary Information** The online version contains supplementary material available at <https://doi.org/10.1007/s00262-022-03268-4>.

**Acknowledgements** The authors thank the patients and parents who contributed samples to the study. Thank you to Jane Cooper, Cay Shakespeare, and Sarah-Jane Staveley for consenting of patients and collection of samples for this study. This work was supported by Cancer Research UK, the Little Princess Trust, Treating Children with Cancer, Amber Phillpott Trust, Birmingham Children's Hospital Research Fund/ Carter the Brave, and the alumni and donors to the University of Birmingham. This work was supported by Phenome Centre Birmingham [MR/M009157/1].

**Author contributions** F.M. and C.D.S. designed the study, supervised research, analysed data, secured funding and wrote the manuscript. F.M. additionally secured ethical approval. V.S. and L.F. designed and performed research. S.B., D.D.S, A.B, U.S., L.G., S.P, M.A., performed research. A.J, G.R.L, A.D.S and W.B.D acquired and interpreted the metabolomics data. P.C. and H.E. gifted BCT-100 and JPH203 respectively. D.P. and F.P. acquired and interpreted the lipidomic profiles. C.C. was chief investigator of the RAAVA clinical trial and provided samples with S.P. K.K. performed and supervised in vivo modelling in the MLL-AF9 model. All authors contributed to writing of the manuscript.

**Funding** This work was supported by Cancer Research UK, the Little Princess Trust, Treating Children with Cancer, Amber Phillpott Trust, Birmingham Children's Hospital Research Fund/ Carter the Brave, and the alumni and donors to the University of Birmingham. This work was supported by Phenome Centre Birmingham [MR/M009157/1].

## Declarations

**Conflict of interests** The authors declare no competing interests.

**Open Access** This article is licensed under a Creative Commons Attribution 4.0 International License, which permits use, sharing, adaptation, distribution and reproduction in any medium or format, as long as you give appropriate credit to the original author(s) and the source, provide a link to the Creative Commons licence, and indicate if changes were made. The images or other third party material in this article are included in the article's Creative Commons licence, unless indicated otherwise in a credit line to the material. If material is not included in the article's Creative Commons licence and your intended use is not permitted by statutory regulation or exceeds the permitted use, you will need to obtain permission directly from the copyright holder. To view a copy of this licence, visit <http://creativecommons.org/licenses/by/4.0/>.

## References

1. Park JH, Riviere I, Gonen M et al (2018) Long-term follow-up of CD19 CAR therapy in acute lymphoblastic leukemia. *N Engl J Med* 378(5):449–459
2. Craddock C, Slade D, De Santo C et al (2019) Combination lenalidomide and azacitidine: a novel salvage therapy in patients who relapse after allogeneic stem-cell transplantation for acute myeloid leukemia. *J Clin Oncol* 37(7):580–588

3. Li S, Tao Z, Xu Y et al (2018) CD33-specific chimeric antigen receptor t cells with different co-stimulators showed potent anti-leukemia efficacy and different phenotype. *Hum Gene Ther* 29(5):626–639
4. Daver N, Garcia-Manero G, Basu S et al (2019) efficacy, safety, and biomarkers of response to azacitidine and nivolumab in relapsed/refractory acute myeloid leukemia: a nonrandomized, open-label phase II study. *Cancer Discov* 9(3):370–383
5. Le Dieu R, Taussig DC, Ramsay AG et al (2009) Peripheral blood T cells in acute myeloid leukemia (AML) patients at diagnosis have abnormal phenotype and genotype and form defective immune synapses with AML blasts. *Blood* 114(18):3909–3916
6. Tang L, Wu J, Li CG et al (2020) Characterization of immune dysfunction and identification of prognostic immune-related risk factors in acute myeloid leukemia. *Clin Cancer Res* 26(7):1763–1772
7. Mussai F, De Santo C, Abu-Dayyeh I et al (2013) Acute myeloid leukemia creates an arginase-dependent immunosuppressive microenvironment. *Blood* 122(5):749–758
8. Toffalori C, Zito L, Gambacorta V et al (2019) Immune signature drives leukemia escape and relapse after hematopoietic cell transplantation. *Nat Med* 25(4):603–611
9. Bronte V, Brandau S, Chen SH et al (2016) Recommendations for myeloid-derived suppressor cell nomenclature and characterization standards. *Nat Commun* 7:12150
10. Azzaoui I, Uhel F, Rossille D et al (2016) T-cell defect in diffuse large B-cell lymphomas involves expansion of myeloid-derived suppressor cells. *Blood* 128(8):1081–1092
11. Pyzer AR, Stroopinsky D, Rajabi H et al (2017) MUC1-mediated induction of myeloid-derived suppressor cells in patients with acute myeloid leukemia. *Blood* 129(13):1791–1801
12. Craddock CF, Houlton AE, Quek LS et al (2017) Outcome of azacitidine therapy in acute myeloid leukemia is not improved by concurrent vorinostat therapy but is predicted by a diagnostic molecular signature. *Clin Cancer Res* 23(21):6430–6440
13. Mussai F, Egan S, Higginbotham-Jones J et al (2015) Arginine dependence of acute myeloid leukemia blast proliferation: A novel therapeutic target. *Blood* 125(15):2386–2396
14. Mussai F, Wheat R, Sarrou E et al (2018) Targeting the arginine metabolic brake enhances immunotherapy for leukaemia. *Int J Cancer* 145:2201–2208
15. Carey A, Edwards DK, Eide CA et al (2017) Identification of interleukin-1 by functional screening as a key mediator of cellular expansion and disease progression in acute myeloid leukemia. *Cell Rep* 18(13):3204–3218
16. Somervaille TC, Cleary ML (2006) Identification and characterization of leukemia stem cells in murine MLL-AF9 acute myeloid leukemia. *Cancer Cell* 10(4):257–268
17. Somervaille TC, Matheny CJ, Spencer GJ et al (2009) Hierarchical maintenance of MLL myeloid leukemia stem cells employs a transcriptional program shared with embryonic rather than adult stem cells. *Cell Stem Cell* 4(2):129–140
18. Salio M, Palmowski M, Atzberger A et al (2004) CpG-matured murine plasmacytoid dendritic cells are capable of in vivo priming of functional CD8 T cell responses to endogenous but not exogenous antigens. *J Exp Med* 199(4):567–579
19. De Santo C, Arscott R, Booth S et al (2010) Invariant NKT cells modulate the suppressive activity of IL-10-secreting neutrophils differentiated with serum amyloid A. *Nat Immunol* 11(11):1039–1046
20. Ather JL, Ckless K, Martin R et al (2011) Serum amyloid A activates the NLRP3 inflammasome and promotes Th17 allergic asthma in mice. *J Immunol* 187(1):64–73
21. Hiratsuka S, Watanabe A, Sakurai Y et al (2008) The S100A8-serum amyloid A3-TLR4 paracrine cascade establishes a pre-metastatic phase. *Nat Cell Biol* 10(11):1349–1355
22. Uchida T, Horiguchi S, Tanaka Y et al (2008) Phase I study of alpha-galactosylceramide-pulsed antigen presenting cells administration to the nasal submucosa in unresectable or recurrent head and neck cancer. *Cancer Immunol Immunother* 57(3):337–345
23. Chang CH, Curtis JD, Maggi LB Jr et al (2013) Posttranscriptional control of T cell effector function by aerobic glycolysis. *Cell* 153(6):1239–1251
24. Jones N, Vincent EE, Cronin JG et al (2019) Akt and STAT5 mediate naive human CD4+ T-cell early metabolic response to TCR stimulation. *Nat Commun* 10(1):2042
25. Hayashi K, Jutabha P, Endou H, Sagara H, Anzai N (2013) LAT1 is a critical transporter of essential amino acids for immune reactions in activated human T cells. *J Immunol* 191(8):4080–4085
26. Lu YC, Parker LL, Lu T et al (2017) Treatment of patients with metastatic cancer using a major histocompatibility complex class II-restricted T-cell receptor targeting the cancer germline antigen MAGE-A3. *J Clin Oncol* 35(29):3322–3329
27. Stroncek DF, Lee DW, Ren J et al (2017) Elutriated lymphocytes for manufacturing chimeric antigen receptor T cells. *J Transl Med* 15(1):59
28. Serafini P, Meckel K, Kelso M et al (2006) Phosphodiesterase-5 inhibition augments endogenous antitumor immunity by reducing myeloid-derived suppressor cell function. *J Exp Med* 203(12):2691–2702
29. Bronte V, Serafini P, De Santo C et al (2003) IL-4-induced arginase 1 suppresses alloreactive T cells in tumor-bearing mice. *J Immunol* 170(1):270–278
30. Corzo CA, Condamine T, Lu L et al (2010) HIF-1alpha regulates function and differentiation of myeloid-derived suppressor cells in the tumor microenvironment. *J Exp Med* 207(11):2439–2453
31. Vasquez-Dunddel D, Pan F, Zeng Q et al (2013) STAT3 regulates arginase-I in myeloid-derived suppressor cells from cancer patients. *J Clin Invest* 123(4):1580–1589
32. Galan-Diez M, Borot F, Mahmood A et al (2022) Subversion of serotonin receptor signaling in osteoblasts by kynurenine driven acute myeloid leukemia. *Cancer Discov* 12(4):1106–1127
33. Witting P, Song C, Hsu K et al (2011) The acute-phase protein serum amyloid A induces endothelial dysfunction that is inhibited by high-density lipoprotein. *Free Radic Biol Med* 51(7):1390–1398
34. Sun L, Zhou H, Zhu Z et al (2015) Ex vivo and in vitro effect of serum amyloid a in the induction of macrophage M2 markers and efferocytosis of apoptotic neutrophils. *J Immunol* 194(10):4891–4900
35. Sander LE, Sackett SD, Dierssen U et al (2010) Hepatic acute-phase proteins control innate immune responses during infection by promoting myeloid-derived suppressor cell function. *J Exp Med* 207(7):1453–1464
36. Tawara I, Kageyama S, Miyahara Y et al (2017) Safety and persistence of WT1-specific T-cell receptor gene-transduced lymphocytes in patients with AML and MDS. *Blood* 130(18):1985–1994
37. Chuc A, Cervantes L, Retiguin F et al (2012) Low number of invariant NKT cells is associated with poor survival in acute myeloid leukemia. *J Cancer Res Clin Oncol* 138(8):1427–1432
38. Boeck C, Amberger D, Doraneh-Gard F et al (2017) Significance of frequencies, compositions, and/or antileukemic activity of (DC-stimulated) invariant NKT, NK and CIK cells on the outcome of patients with AML. *ALL and CLL J Immunother* 40(6):224–248

39. De Lalla C, Rinaldi A, Montagna D et al (2011) Invariant NKT cell reconstitution in pediatric leukemia patients given HLA-haploidentical stem cell transplantation defines distinct CD4+ and CD4- subset dynamics and correlates with remission state. *J Immunol* 186(7):4490–4499
40. Metelitsa LS, Weinberg KI, Emanuel PD, Seeger RC (2003) Expression of CD1d by myelomonocytic leukemias provides a target for cytotoxic NKT cells. *Leukemia* 17(6):1068–1077
41. Jahnke S, Schmid H, Secker KA et al (2019) Invariant NKT cells from donor lymphocyte infusions (DLI-iNKTs) promote ex vivo lysis of leukemic blasts in a CD1d-dependent manner. *Front Immunol* 10:1542
42. Rotolo A, Caputo VS, Holubova M et al (2018) Enhanced anti-lymphoma activity of CAR19-iNKT Cells Underpinned by dual CD19 and CD1d targeting. *Cancer Cell* 34(4):596–610.e11
43. Thapa P, Arocha S, Chung J et al (2017) Histone deacetylase 3 is required for iNKT cell developments. *Sci Rep* 7(1):5784
44. De Santo C, Salio M, Masri SH et al (2008) Invariant NKT cells reduce the immunosuppressive activity of influenza A virus-induced myeloid-derived suppressor cells in mice and humans. *J Clin Invest* 118(12):4036–4048
45. Kamaladasa A, Wickramasinghe N, Adikari TN et al (2016) Expansion of highly activated invariant natural killer T cells with altered phenotype in acute dengue infection. *Clin Exp Immunol* 185(2):228–238
46. Innamarato P, Kodumudi K, Asby S et al (2020) Reactive myelopoiesis triggered by lymphodepleting chemotherapy limits the efficacy of adoptive T cell therapy. *Mol Ther* 28(10):2252–2270

**Publisher's Note** Springer Nature remains neutral with regard to jurisdictional claims in published maps and institutional affiliations.